Combinatorial Chemistry & High Throughput Screening, 2020, *23*, 611-623

RESEARCH ARTICLE

New Platinum (II) Ternary Complexes of Formamidine and Pyrophosphate: Synthesis, Characterization and DFT Calculations and *In vitro* Cytotoxicity

Ahmed A. Soliman[1,*], Fawzy A. Attaby[1], Othman I. Alajrawy[1,2], Azza A.A. Abou-hussein[3] and Wolfgang Linert[4]

[1]*Department of Chemistry, Faculty of Science, Cairo University, Giza 12613, Egypt;* [2]*Department of Applied Chemistry, College of Applied Science, University of Fallujah, Fallujah, Anbar, Iraq;* [3]*Faculty of Women for Arts, Science and Education, Ain Shams University, Heliopolis, Cairo, Egypt;* [4]*Institute of Applied Synthetic Chemistry, Vienna University of Technology, Getreidemarkt 9-163-AC, Vienna A-1060, Austria*

Abstract: ***Aim and Objective*:** Platinum (II) and platinum (IV) of pyrophosphate complexes have been prepared and characterized to discover their potential as antitumor drugs. This study was conducted to prepare and characterize new ternary platinum (II) complexes with formamidine and pyrophosphate as an antitumor candidate.

***Materials and Methods*:** The complexes have been characterized by mass, infrared, UV-Vis. spectroscopy, elemental analysis, magnetic susceptibility, thermal analyses, and theoretical calculations. They have been tested for their cytotoxicity, which was carried out using the fast-colorimetric assay for cellular growth and survival against MCF-7 (breast cancer cell line), HCT-116 (colon carcinoma cell line), and HepG-2 (hepatocellular cancer cell line).

***Results*:** All complexes are diamagnetic, and the electronic spectral data displayed the bands due to square planar Pt(II) complexes. The optimized complexes structures (**1-4**) indicated a distorted square planar geometry where O-Pt-O and N-Pt-N bond angles were 82.04°-96.44°, respectively. Results also show that all complexes are neutral, stable and non-hygroscopic and have noticeable cytotoxicity with IC_{50} (μM): 0.035-0.144 MCF-7(breast cancer cell line), 0.042-0.187 HCT-116 (colon carcinoma cell line), and 0.063-0.168 HepG-2 (hepatocellular cancer cell line). Moreover, the results show that the complex (**4**) has the best IC_{50} value.

***Conclusion*:** The complexes showed noticeable cytotoxicity and are considered as promising antitumor candidates for further applications.

ARTICLE HISTORY

Received: April 26, 2019
Revised: August 02, 2019
Accepted: August 18, 2019

DOI:
10.2174/1386207323666200218115700

Keywords: Pt(II), pyrophosphate, formamidine, antitumor, spectroscopy, thermal analysis, magnetic and MO calculations.

1. INTRODUCTION

Metal-Organic compounds have been used in medicinal chemistry for many reasons. The most important of these reasons are their lipophilic nature and their ability to provide a huge variety of functionalized organic ligands [1]. The applications of transition metal complexes as anticancer reagents are beneficial [2-6]. The metal complexes with ligands bearing O, N donor atoms of organic structures have been studied for their medicinal applications [7]. Mixed ligand metal complexes are the most interesting because they contain different moieties with enhanced properties [8, 9]. The design of thermally stable complexes that can reach the target position is the aim behind the preparation of these complexes.

On the other hand, the complexes should be unreactive towards the reducing agent glutathione (GSH) and extra- and intracellular biomolecules, which are present in most cells [10]. At present, platinum (II) complexes are used in 50 to 70% of all chemotherapy schemes administered to cancer patients [8, 11]. Nevertheless, the use of cisplatin and interrelated drugs (carboplatin and oxaliplatin) is unsatisfactory by their dose-limiting harmful side effects and by acquired resistance on long therapy as well as by their lack of efficiency against various cancer types, specifically

*Address correspondence to this author at the Department of Chemistry, Faculty of Science, Cairo University, Giza 12613, Egypt;
Tel: 002 01110121379; Fax: 002 02 35676556;
E-mail: ahmedsoliman61@gmail.com

1875-5402/20 $65.00+.00

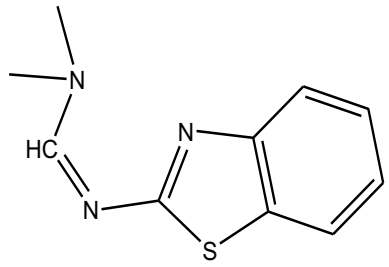

(Z)-N'-(benzo[d]thiazol-2-yl)-N,N-dimethylformamidine

(**L1**)

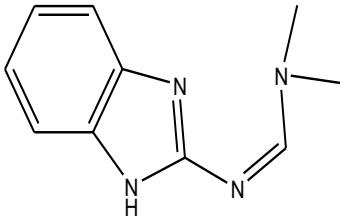

(Z)-N'-(1H-benzo[d]imidazol-2-yl)-N,N-dimethylformamidine

(**L2**)

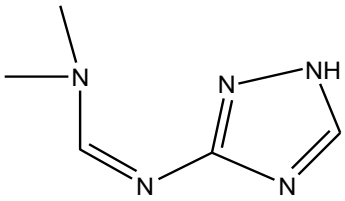

(Z)-N,N-dimethyl-N'-(1H-1,2,4-triazol-3-yl)formamidine

(**L3**)

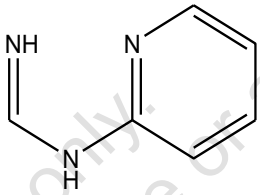

N-(pyridin-2-yl)formamidine

(**L4**)

Fig. (1). Structures of the formamidine ligands (L1-L4).

metastatic ones [12]. Recently, many cobalt, nickel, and palladium mono and binuclear pyrophosphate complexes showed noteworthy inhibition against ovarian tumor cell lines [13]. Platinum (II) and platinum (IV) of pyrophosphate complexes have been prepared and characterized to discover their potential as antitumor drugs [14]. Furthermore, formamidine ligands under study (L_1-L_4) have proven to have good cytotoxic activity [15]. In continuation of our previous work on formamidine complexes [15-19], we report our investigations of platinum (II) mixed complexes with formamidine and pyrophosphate ligands as potential chemotherapeutics agents. The formamidine ligand structures are given in Fig. (**1**).

2. MATERIALS & METHODS

2.1. Materials

The chemicals used are highly pure. Potassium tetrach loroplatinate (II), $K_2[PtCl_4]$ and sodium pyrophosphate decahydrate $Na_2P_2O_7.10H_2O$ were purchased by Aldrich. The solvents used were of analytical grade.

2.2. Measurements

The carbon, hydrogen and nitrogen's elemental analyses were analyzed at the microanalytical center of Cairo University, Egypt. Infrared measurements were carried out on solids as KBr discs using Jasco FTIR-460 plus and Jasco FTIR-4000 (ranging 400-4000 cm^{-1}) and mass spectrometric analyses have been carried out using GCMS-QP1000EX Shimadzu (electron ionization). UV-Vis. spectra have been conducted by Optizen UV-Vis. spectrophotometer. The ^{1}HNMR spectra are carried out using Spectrospin-Bruker-AC 200 MHz NMR Spectro-meter (L_1) and Varian NMR 400 (Complex **1**). Samples were dissolved in DMSO using tetramethyl-silane (TMS) as an internal reference. The susceptibility of the solid complexes was measured by Sherwood Scientific magnetic susceptibility balance. Thermal analyses have been conducted using a Shimadzu thermo-gravimetric analyzer TGA-60H (20 mL / min N_2 atmosphere, rate of 10°C / min from 25°C).

2.3. Synthesis of Complexes

2.3.1. Synthesis of Ternary Pt(II) Complexes

The formamidine ligands were prepared by our group and are published in the previous work [15]. The ternary complexes have been prepared following a similar procedure to that reported by our group [15-19]; 1.0 mmol (0.42 g) of K_2PtCl_4, 1.0 mmol (0.45 g) of sodium pyrophosphate decahydrate $Na_4P_2O_7.10H_2O$ were separately dissolved in water (10 mL at 50°C). 1.0 mmol; of **L1** (0.21 g) (L_1 = (Z)-N'-(benzo[d]thiazol-2-yl)-N, N-dimethylformamidine), **L2** (0.19 g) (L_2 = (Z)-N'-(1H-benzo[d]imidazol-2-yl)-N,N-dimethylformamidine), **L3** (0.14 g) (L_3 = (Z)-N,N-dimethyl-N'-(1H-1,2,4-triazol-3-yl) formamidine) and **L4** (0.12 g) (L_4 = N-(pyridin-2-yl)formamidine) were separately dissolved in ethyl alcohol (10 mL) and mixed with the aqueous solution (10 mL) of Pt(II) salt slightly with constant stirring. Then, the pyrophosphate solution was added to the mixture slightly under constant stirring. The whole mixture was adjusted to pH 8 and refluxed at 90°C for 15 hours under constant stirring [16]. The green solid complexes were purified using DMSO. The complexes obtained were $[Pt(L_1)PPi].2H_2O$ (**1**) (0.38 g; yield: 61.7%), $[Pt(L_2)PPi].2H_2O$ (**2**) (0.36 g; yield: 59.7%), $[Pt(L_3)PPi].2H_2O$ (**3**) (0.37 g; yield: 68.3%) and $[Pt(L_4)PPi].7/2H_2O$ (**4**) (0.34 g; yield: 61.8%). The elemental analysis of complexes included *Anal. Calc. for (**1**); ($C_{10}H_{17}N_3O_9P_2PtS$, Calc.: C,* 19.61*; H,* 2.80*; N,* 6.86*, Found: C,* 19.45*; H,* 2.64*; N,* 6.49*%), (**2**)($C_{10}H_{18}N_4O_9P_2Pt$, Calc.:* C, 20.18; H, 3.05; N, 9.41, *Found:* C, 19.98; H, 2.98; N, 9.23 *%), (**3**)($C_5H_{15}N_5O_9P_2Pt$, Calc.:* C,

Table 1. The analytical and spectroscopic data of the synthesized Pt(II) pyrophosphate complexes (1-4).

Complexes	Molar Mass	Color	Solubility	Λ_m $Ohm^{-1} cm^2 mol^{-1}$	UV-Vis. Absorption Peaks (nm)	Assignment
$[Pt(L_1)PPi].2H_2O$ (1)	612.35	Green	DMSO	5.44	330-340 375 445-460 500	π - π * n- π MLCT $^1A_{1g} \rightarrow {}^3B_{1g}$
$[Pt(L_2)PPi].2H_2O$ (2)	595.30	Green	DMSO	3.67	310-330 350 410-440 500	π - π * n- π * MLCT $^1A_{1g} \rightarrow {}^3B_{1g}$
$[Pt(L_3)PPi].2H_2O$ (3)	546.23	Green	NS	-	NS	-
$[Pt(L_4)PPi].7/2H_2O$ (4)	556.26	Green	DMSO	3.45	300-325 350-385 400 460	π - π * n- π * MLCT $^1A_{1g} \rightarrow {}^3B_{1g}$

10.99; H, 2.77; N, 12.82, *Found:* C, 10.80; H, 2.64; N, 12.71 *%) and (4)* ($C_6H_{16}N_3O_{10.5}P_2Pt$, *Calc*.: C, 12.98; H, 2.90; N, 7.57. *Found*: C, 12.73; H, 2.72; N, 7.45).

2.4. Evaluation of the Antitumor Activity

The cytotoxicity test was performed using the fast-colorimetric assay for cellular growth and survival [20]. The human tumor cells used were MCF-7 (breast cancer cell line), HCT-116 (colon carcinoma cell line), and HepG-2 (hepatocellular cancer cell line) to test the cytotoxicity of the complexes under study. The tumor cells were cultivated in Dulbecco's modified Eagle's medium (DMEM) or RPMI-1640 dependent on the type of tumor cell line added with 10% of heat-inactivated fetal bovine serum, 1% L-glutamine, HEPES buffer and 50µg/ml gentamycin. The media were incubated at 37ºC in a humidified atmosphere with 5% CO_2 and were sub-cultured twice a week throughout the tests. Each test was carried out in a triplicate experiment. The cytotoxicity was tested in the Al-Azhar University Regional Centre for Mycology and Biotechnology, Cairo, Egypt.

3. RESULTS AND DISCUSSION

The prepared Pt(II) complexes (**1-4**) analytical and spectral parameters are given in Table **1**. All the Pt(II) complexes are stable and non-hygroscopic and soluble DMSO. The data of elemental analyses are in good agreement with those of the suggested structures of the complexes (the experimental part).

3.1. Infrared Spectral Study

The most important IR peaks of prepared Pt(II) complexes are presented (Table **2**). The strong bands that appeared in ligands at 1600-1642 cm^{-1} are assigned to the azomethine ν(C=N) and at 1261-1276 cm^{-1} are due to ν(C-N) [13, 15-22]. In the spectra of the investigated complexes, the above-mentioned bands are shifted to 1631-1634 cm^{-1} and 1254-1277 cm^{-1}; respectively. Additional bands are observed for the pyrophosphate ligand at (1210-1228 cm^{-1}) assigned to $\nu(PO_2)$, at (883-976 cm^{-1}) and (718-763 cm^{-1}) assigned to the asymmetric and symmetric stretching vibration of the P-O-P bridge, respectively. The asymmetric and symmetric stretching frequencies of the terminal $\nu(PO_3)$ bands observed at (1112-1123 cm^{-1}) indicate that the $[P_2O_7]^{-4}$ implements a bent structure [13, 23, 24]. New bands at (455-495 cm^{-1}) and at (597-609 cm^{-1}) were assigned to ν(M-N) and ν(M-O); respectively. Furthermore, the infrared spectra of the complexes (**1-4**) showed the bands of hydrated water at the range of (3419-3431 cm^{-1}). The experimental and calculated IR bands of complex (**2**) are shown in Fig. (**2**). The calculated and experimental data are covenant as shown in Table **2** with a relative error of 0.00-10.96%. This error may be originated from the dissimilar methodology used to get the data; the experimental data are measured in the solid-state while the theoretical data are obtained for an isolated molecule, which is expected to be close to that in the gaseous state.

3.2. Mass Spectra

The key fragmentations in the mass spectra of the produced complexes are recorded in Table **3**. Complex (**1**) (M.Wt = 612.35) showed peaks at m/z = 612 (M; parent), m/z = 586 (M-$2H_2O$), m/z = 421 (M-($2H_2O$, P_2O_6)), m/z = 212 (PtO), m/z = 204 (L_1) and m/z = 154 (P_2O_6). Complex (**2**) (M.Wt = 595.30) gave peaks at m/z = 594 (M; parent), m/z = 559 (M-$2H_2O$), m/z = 418 (M- P_2O_7), m/z = 407 (M-L_2), and m/z = 182 (L_2). Complex (**3**) (M.Wt = 547.23) gave peaks at m/z = 546 (M; parent), m/z = 404 (M-P_2O_4), m/z = 375 (M-($2H_2O$, L_3)), m/z = 236 (M-($2H_2O$, $2CO_2$)) and m/z = 140 (L_3). Complex (**4**) (M.Wt = 555.23) gave peaks at m/z = 556 (M; parent), m/z = 537 (M-H_2O), m/z = 507 (M-$7/2H_2O$), m/z = 430 (M-L_4), and m/z = 120 (L_4). The spectra of the complexes (**1-4**) also showed peaks at 193, 194 and 195 m/z which are assigned to the stable platinum isotopes

Table 2. Most characteristic observed and calculated vibrational frequencies cm^{-1} for Pt(II) complexes.

Compound	Obs.	Calc.	% Relative Error	Assignment
[Pt(L_1)PPi].$2H_2O$ (1)	3431	-	-	υ(O-H)Hydrated
	1631	1677	2.82	υ(C=N) imin.
	1271	1264	0.55	υ(C-N)
	973as 747s	867 826	10.89 10.57	υ(P-O-P)brid.
	1117as 1062s	1110 1098	0.62 3.38	υ(PO_3)
	600	605	0.83	υ(M-O)
	437	457	4.57	υ(M-N)
[Pt(L_2)PPi].$2H_2O$ (2)	3425	-	-	υ(O-H)Hydrated
	1633	1720	5.32	υ(C=N) imin.
	1277	1257	1.56	υ(C-N)
	973as 757s	867 840	10.89 10.96	υ(P-O-P)brid.
	1123as 1058s	1111 1037	1.06 1.98	υ(PO_3)
	611	607	0.65	υ(M-O)
	447	455	1.78	υ(M-N)
[Pt(L_3)PPi].$2H_2O$ (3)	3419	-	-	υ(O-H)Hydrated
	1634	1710	4.65	υ(C=N) imin.
	1214	1248	2.80	υ(C-N)
	976as 718s	864 740	11.47 3.06	υ(P-O-P)brid.
	1114as 1058s	1092 1064	1.97 0.56	υ(PO_3)
	618	609	1.45	υ(M-O)
	487	495	1.64	υ(M-N)
[Pt(L_4)PPi].7/$2H_2O$ (4)	3428	-	-	υ(O-H)Hydrated
	1629	1739	6.75	υ(C=N) imin.
	1254	1260	0.47	υ(C-N)
	883as 763s	870 826	1.47 8.25	υ(P-O-P)brid.
	1112as 1055s	1108 1028	0.35 2.55	υ(PO_3)
	597	597	0.00	υ(M-O)
	452	479	5.97	υ(M-N)

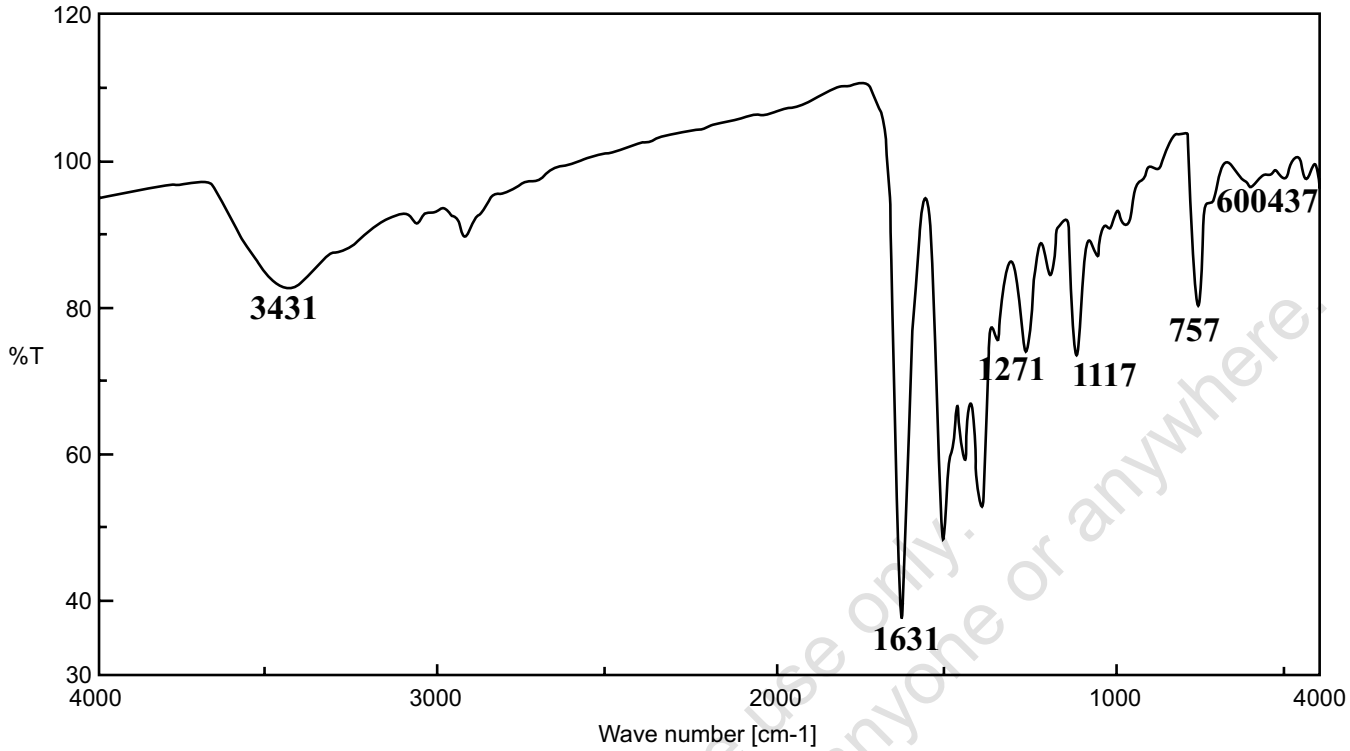

Fig. (2). The IR spectrum of [Pt(L_1)PPi].2H_2O (**1**).

Table 3. Characteristic mass fragmentations data of Pt(II) complexes.

Complex	Molar Mass	Important Mass Fragmentations (m/z) Values
[Pt(L_1)PPi].2H_2O (1)	612.35	612 (M), 586 (M-2H_2O), 421 (M-2H_2O, P_2O_6), 371 (M-L_1), 204 (L_1), 212 (PtO), 154 (P_2O_6) Pt isotopes 193, 194, 195
[Pt(L_2)PPi].2H_2O (2)	595.30	594 (M), 559 (M-2H_2O), 418 (M-P_2O_7), 407 (M-L_2), 182 (L_3), Pt isotope 194
[Pt(L_3)PPi].2H_2O (3)	547.23	546 (M), 404 (M-P_2O_4), 375 (M-(2H_2O, L_3)), 140 (L_3), Pt isotopes 193, 194, 195
[Pt(L_4)PPi].7/2H_2O (4)	555.23	556 (M^{+1}), 537 (M-H_2O), 507 (M-7/2H_2O), 430 (M-L_4), 120 (L_4), Pt isotopes 194, 195

[24]. The results also indicate the monomeric nature of the investigated complexes.

3.3. Electronic Spectra

The measurements of the absorption spectra the complexes (**1**, **2**, **4**) were conducted in DMSO at 200-1100 nm. The resulting data are listed in Table **1**. The spectra exhibited two bands at 300-340 nm and 350-385 nm, which is due to the $\pi\rightarrow\pi^*$ and $n\rightarrow\pi^*$ transitions of the aromatic rings and the azomethines of the ligands; respectively [25]. The shoulders at 400-460 nm are due to metal to ligand charge transfer (LMCT) in the square planar species, which is supported by the DFT calculations (*vide infra*). The d-d transition within the low spin square planar platinum (II) (d^8) species has been shown as a broad band at 460-500 nm due to $^1A_{1g} \rightarrow {}^3B_{1g}$ transition [25, 26]. The configurations of the calculated main excitation electronic transition, as well as the oscillator strength of Pt(II) pyrophosphate complexes, are represented in Table **4**. The calculated transitions are covenant with the experimental ones. Complex (**1**) is presented in Fig. (**3**). The calculated orbital excitations were deduced from HOMO and LUMO energies.

3.4. The ^{1}H NMR Spectra

The ^{1}HNMR spectrum of complex (**1**) has been measured; as a representative example to emphasize that the complexes are diamagnetic confirming the magnetic susceptibility measurements (*vide infra*); Fig. (**4**). Complex (**1**) showed a singlet band at 8.62 ppm (integrated to 1 proton), which is assigned to the aldimine =CH.

The complex also showed multiplet peaks at 6.94-7.20 ppm (integrated to 4 protons) assigned to the benzothiazole moiety and multiplet peaks at 2.65-3.33 ppm (integrated to 6 protons) assigned to the two CH_3 groups. The CH_3 multiplet peaks were found to be slightly shifted from those of the ligand (L_1) due to the participation of benzothiazole nitrogen and the N-$(CH_3)_2$ nitrogen in coordination (ligand (L_1): 8.37 ppm (1H;=CH aldimine), 7.17-7.71(4H;Ph) and 3.08-3.13 (6H; 2CH_3)).

Table 4. Computed main excitation energies nm(eV), electronic transition configurations of Pt(II) complexes.

Complex	nm(eV)	Exp nm	Composition (>10%)
[Pt(L_1)PPi].2H_2O (1)	339(3.648)	330	HOMO-9→LUMO(60%), HOMO-7→LUMO +1(25%), HOMO→LUMO+1(15%)
	347(3.571)	340	HOMO-8→LUMO(45%), HOMO-7→LUMO (38%), HOMO-6→LUMO(13%)
	369(3.358)	375	HOMO-6→LUMO(51%), HOMO-5→LUMO (36%), HOMO-9→LUMO(13%)
	441(2.807)	445	HOMO-1→ LUMO(42%), HOMO-4→LUMO (37%), HOMO-8→LUMO(16%)
	463(2.677) 473(2.620)	460	HOMO-2→LUMO(50%), HOMO-1→LUMO (33%), HOMO-3→LUMO(26%) HOMO-4→LUMO(49%), HOMO-1→LUMO (38%), HOMO-1→LUMO(14%)
	504(2.460)	500	HOMO→LUMO(67%), HOMO-1→LUMO(14%)
[Pt(L_2)PPi].2H_2O (2)	315(3.933)	310	HOMO-7→LUMO(53%), HOMO-9→LUMO(43%)
	325(3.814)	330	HOMO-7→LUMO(41%), HOMO-6→LUMO (41%), HOMO-5→LUMO(17%)
	415(2.981)	410	HOMO→LUMO(49%), HOMO-2→LUMO (44%).
	429(2.885)	440	HOMO-2→LUMO(47%), HOMO-1→LUMO (43%).
	443(2.795)	500	HOMO-1→LUMO(51%), HOMO→LUMO (41%).
[Pt(L_3)PPi].2H_2O (3)	338(3.66)	-	HOMO-2→LUMO+1(44%), HOMO-1→LUMO+1(42%), HOMO-→LUMO(14%)
	356(3.482)	-	HOMO-1→LUMO(54%), HOMO→LUMO (30%), HOMO-2→LUMO+1(14%)
	381(3.249)	-	HOMO→LUMO (59%), HOMO-1→LUMO (33%).
[Pt(L_4)PPi].7/2H_2O (4)	313(3.982)	300	HOMO-3→LUMO(53%), HOMO-4→LUMO (30%).
	319(3.881)	315	HOMO-1→LUMO+2(45%), HOMO-1→LUMO+1(30%), HOMO→LUMO+2(22%).
	324(3.823)	325	HOMO→LUMO+1(45%),HOMO→LUMO+2(27%),HOMO-1→LUMO+2(20%).
	363(3.406)	350	HOMO-1→LUMO (43%), HOMO-2→LUMO(41%).
	370(3.356)	385	HOMO-2→LUMO(50%), HOMO-1→LUMO (40%).
	399(3.101)	400	HOMO-1→LUMO (46%), HOMO→LUMO(44%).
	410(3.020)	460	HOMO-2→LUMO (58%), HOMO-1→LUMO(37%).
	428(2.895)		HOMO→LUMO (53%), HOMO-1→LUMO(34%).

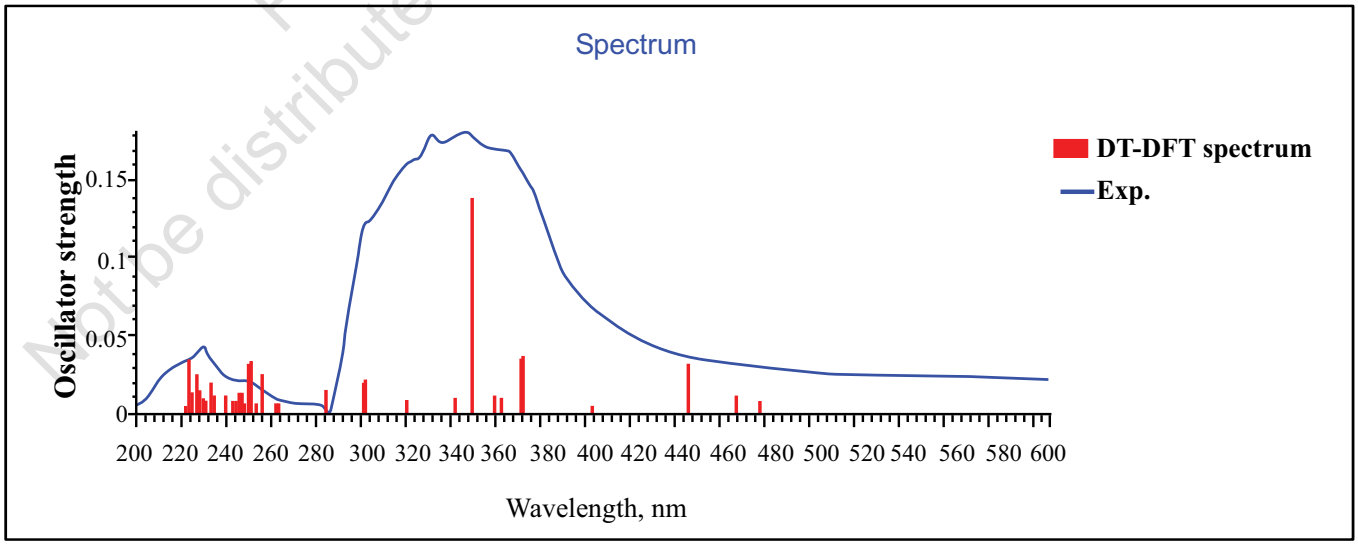

Fig. (3). Contd…

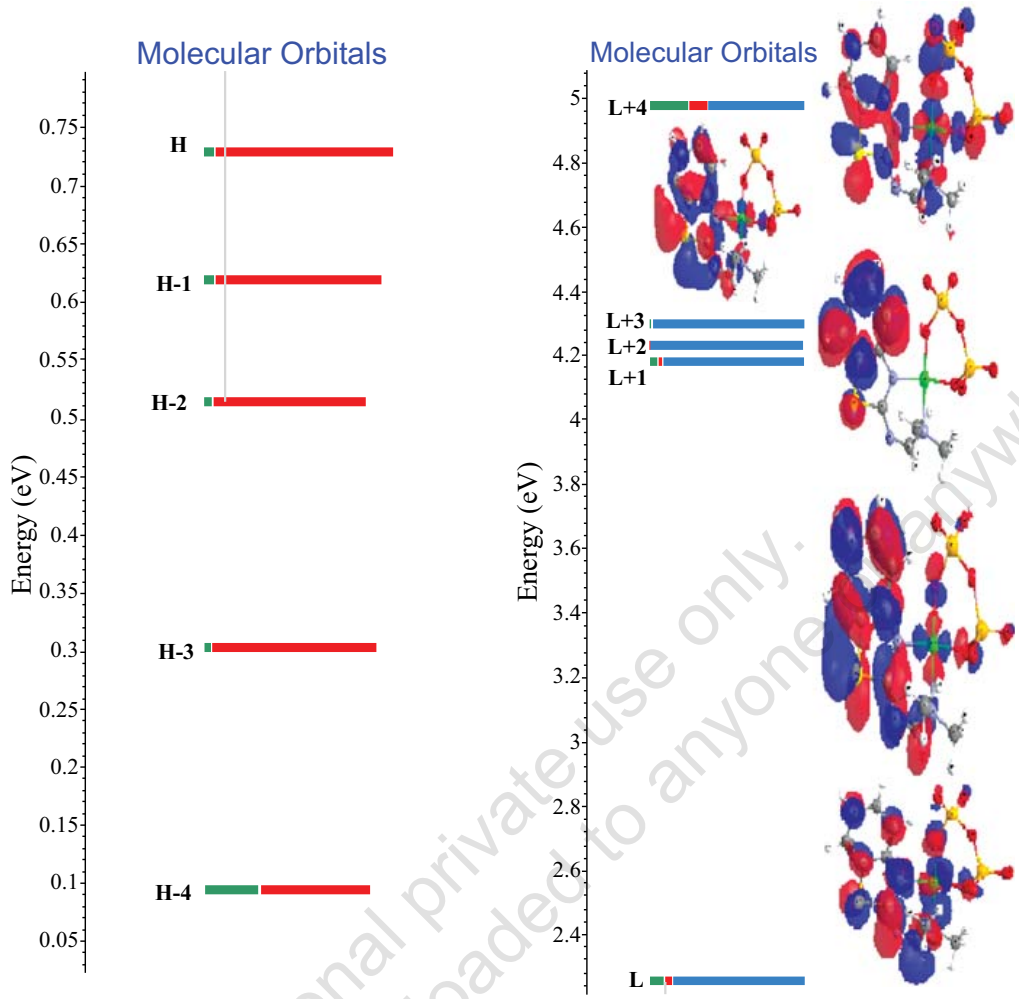

Fig. (3). The experimental and TD-DFT calculated UV-visible spectra of complex (**1**) experimental (red line), calculated (blue line) and the molecular orbitals HOMOs, and LUMOs percent) (isovalue=0.02). *(A higher resolution / colour version of this figure is available in the electronic copy of the article).*

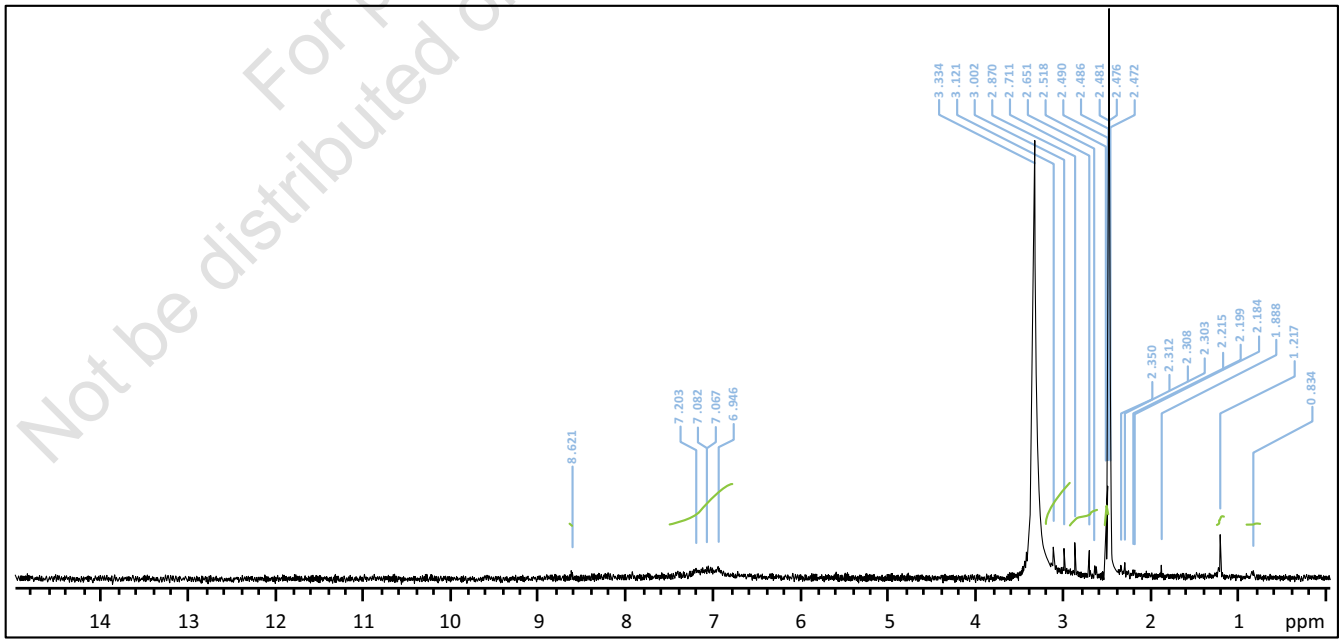

Fig. (4). ^{1}HNMR spectrum of [Pt(L_1)PPi].2H_2O (**1**). *(A higher resolution / colour version of this figure is available in the electronic copy of the article).*

Table 5. Thermogravimetric analytical data for decomposition of Pt(II) complexes.

Complex	Molar Mass	TG Range (K)	DTA $_{max}$ (K)	Mass Loss Found (Cal.%)	Assignment of the Removed Species	Metallic Residue Found (Cal.%)
$[Pt(L_1)PPi].2H_2O$ (1)	612.35	303-512 512-746 746-1259	410 541 759	5.84%; (5.87%) 23.29%; (23.52%) 35.93%; (36.09%)	$[2H_2O]$ $[P_2O_5]$ $[C_{10}H_{11}N_3S, O_2]$	PtO 33.01 (34.45)
$[Pt(L_2)PPi].2H_2O$ (2)	595.30	292-502 502-683 683-872	544 678 710	5.45%; (6.04%) 28.62%; (29.22%) 35.78%; (36.95%)	$[2H_2O]$ $[P_2O_7]$ $[C_{10}H_{12}N_4]$	Pt 30.15 (32.75)
$[Pt(L_3)PPi].2H_2O$ (3)	546.23	297-447 447-794 794-1137	586 723 994	6.48%; (6.59%) 24.79%; (25.99%) 30.98%; (31.30%)	$[2H_2O]$ $[P_2O_5,N(CH_3)_2]$ $[C_3H_3N_4, O_2]$	Pt 37.72 (35.69)
$[Pt(L_4)PPi].7/2H_2O$ (4)	555.23	298-384 384-709 709-928	339 684 722	3.11%; (3.24%) 33.52%; (33.67%) 26.99%; (27.55%)	$[H_2O]$ $[5/2H_2O, P_2O_5]$ $[C_6H_7N_3, O_2]$	Pt 36.38 (35.12)

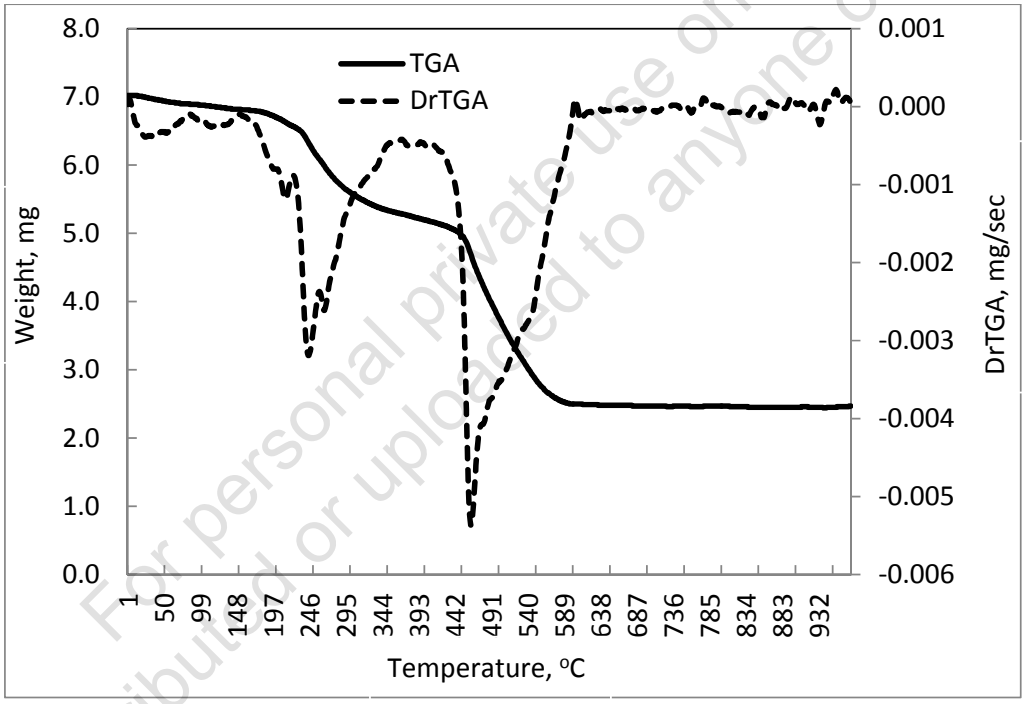

Fig. (5). The thermogram of $[Pt(L_1)PPi].2H_2O$ **(1)**.

3.5. Magnetic Susceptibility

The magnetic measurement of platinum (II) complexes (**1-4**) indicated that the complexes are diamagnetic, which is due to the divalent state of Pt(II) with d^8 electronic configuration ($e_g^4\ b_{2g}^2\ a_{1g}^2$) in a square planar geometry where electrons are paired [27].

3.6. Thermal Analysis

The thermogravimetric analysis (TGA) was performed to explore the thermal stability of the complexes. The first derivative of the thermogram plots (DrTGA) was also used to precisely determine the range of each step. The decomposition data are specified in Table **5**. The assignments of the different decomposed steps are in consistent with the complexes formulae. The thermograms of complexes (**1**) as an example is shown in Fig. (**5**). The thermodynamic parameters were calculated using the Integral method of Coats–Redfern and the approximated method of Horowitz-Metzger [28, 29] considering the Ozawa correction [30]. The values of the thermodynamic parameters are listed in Table **6**. The complexes are stable as indicated by their moderately high total activation energy (368-660 kJ mol^{-1}). The variation in the sign of the entropy (ΔS^*) may be explained by the difference in the structural complexities (organization and/or arrangement) of the complexes in the activation state, which stands as the reactant to the next step [31, 32].

Table 6. Data of the thermodynamic parameters of the thermal decomposition of Pt(II) complexes.

Complex	Decomposition Temperature (K)	ΔE / KJ mol^{-1}	R2	ΔS / J K^{-}1 mol^{-1}	ΔH / KJ mol^{-1}	ΔG / KJ mol^{-1}
[Pt(L_1)PPi].2H_2O (1)	303-508 508-740 740-889	63 158 377	0.97 0.97 0.92	-97 29 229	60 154 371	100 138 198
		498		**355**	**558**	**436**
[Pt(L_2)PPi].2H_2O (2)	295-635 635-692 692-775	74 356 240	0.96 0.96 0.87	-114 266 68	69 350 234	132 169 186
		660		**220**	**635**	**478**
[Pt(L_3)PPi].2H_2O (3)	297-455 455-563 568-713 710-1027	57 124 216 263	0.99 0.98 0.94 0.85	-96 -22 103 96	54 120 211 257	88 131 151 187
		660		**81**	**642**	**557**
[Pt(L_4)PPi].7/2H_2O (4)	298-384 384-709 709-928	56 100 212	0.95 0.95 0.85	-92 115 33	53 94 205	84 173 182
		368		**56**	**352**	**439**

Table 7. Equilibrium geometric parameters bond lengths (Å), bond angles (°) and dihedral angles (°) of optimized Pt(II) complexes by using DFT/B3LYP/LanL2DZ basis set.

[Pt(L_1)PPi].2H_2O (1)	Bond Lengths Å	Bond Angles°	
Pt(18)-O(3)	2.031	O(3)-Pt(18)O(4)	90.52
Pt(18)-O(4)	2.020	O(3)-Pt(18)-N(13)	91.38
Pt(18)-N(13)	2.053	O(4)-Pt(18)-N(19)	89.29
Pt(18)-N(19)	2.135	N(13)-Pt(18)-N(19)	88.86
-	-	O(3)-Pt(18)-N(19)	179.12
-	-	O(4)-Pt(18)-N(13)	175,39
[Pt(L_2)PPi].2H_2O (2)	-	-	-
Pt(18)-O(3)	2.036	O(3)-Pt(18)O(4)	92.39
Pt(18)-O(4)	2.037	O(3)-Pt(18)-N(13)	90.57
Pt(18)-N(13)	2.036	O(4)-Pt(18)-N(19)	83.12
Pt(18)-N(19)	2.11	N(13)-Pt(18)-N(19)	93.99
-	-	O(3)-Pt(18)-N(19)	175.32
-	-	O(4)-Pt(18)-N(13)	174.94
[Pt(L_3)PPi].2H_2O (3)	-	-	-
Pt(1)-O(12)	2.056	O(12)-Pt(1)O(13)	92.11
Pt(1)-O(13)	2.051	O(12)-Pt(1)-N(2)	82.04
Pt(1)-N(2)	1.968	O(13)-Pt(1)-N(7)	85.04
Pt(1)-N(7)	2.109	N(13)-Pt(18)-N(19)	91.79
-	-	O(12)-Pt(1)-N(7)	173.83
-	-	O(13)-Pt(1)-N(2)	176.80
[Pt(L_4)PPi].7/2H_2O(4)	-	-	-
Pt(1)-O(2)	2.047	O(2)-Pt(1)O(3)	96.44
Pt(1)-O(3)	2.032	O(2)-Pt(1)-N(8)	88.66
Pt(1)-N(8)	2.048	O(3)-Pt(1)-N(14)	82.04
Pt(1)-N(14)	1.970	N(8)-Pt(1)-N(14)	92.82
-	-	O(2)-Pt(1)-N(14)	178.46
-	-	O(3)-Pt(1)-N(8)	174.34

3.7. Computational Studies

The optimized geometries of the complexes (**1-4**) using Density functional theory DFT with B3LYP / LanL2DZ basis set [33, 34] are shown in Fig. (**6**). The relevant bond angles and the bond lengths are given in Table **7**. The transition energy of the complexes was calculated from the time-dependent TD-DFT (time-dependent density functional linear response theory). The angles of Pt(II)-formamidine and pyrophosphate ligands vary from (82.04° to 96.44°) indicating distorted square planar structures [32]. The O-Pt-O bond angles (90.52°-96.44°) are comparable with the platinum (II) diamine pyrophosphate complexes in pyroen-2 (en = 1,2-ethanediamine) and pyrodach-2 (dach = trans-1,2-cyclohexanediamine) (91.33°-96.20°) [14]. The N-Pt-N bond

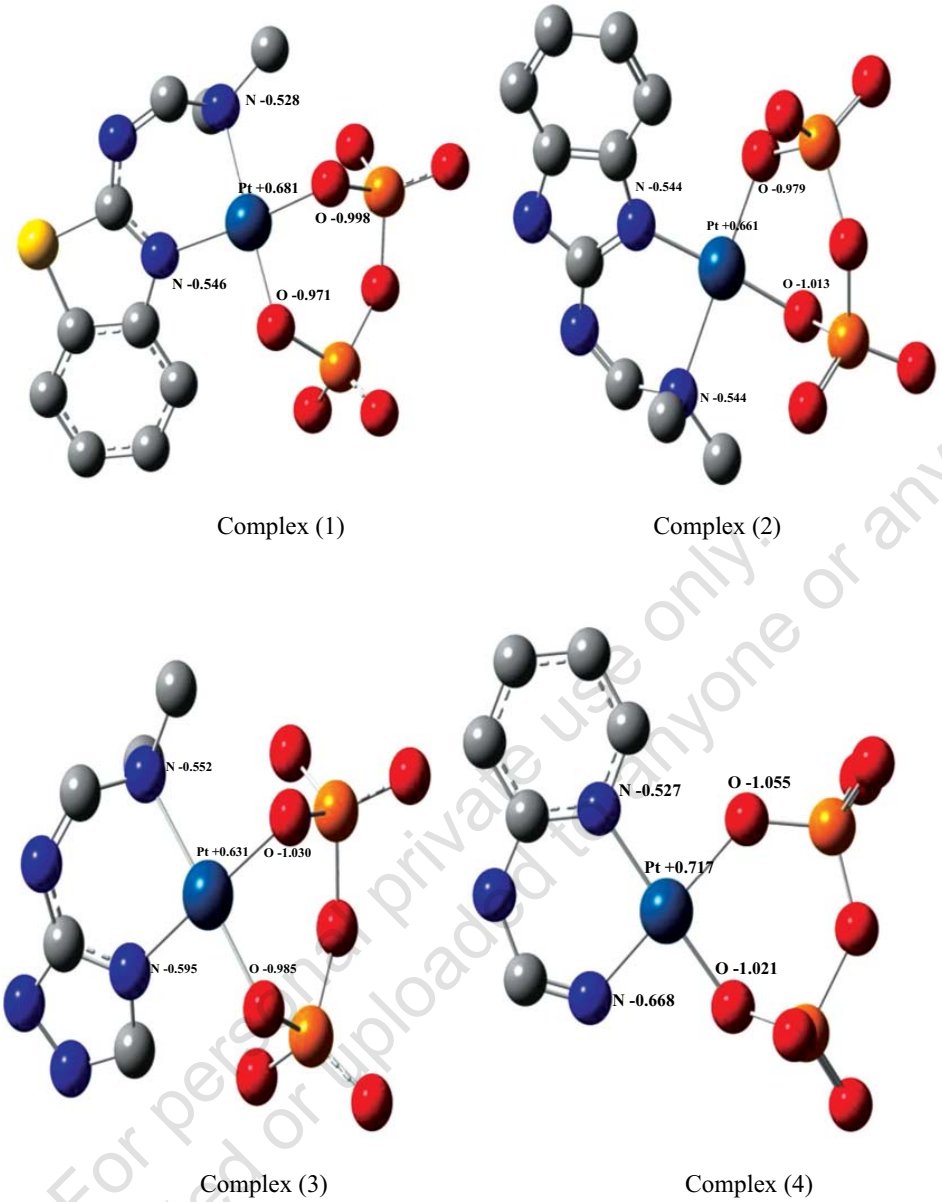

Complex (1) Complex (2)

Complex (3) Complex (4)

Fig. (6). Optimized molecular structures and atomic charges of ternary Pt(II) complexes; Carbon (gray), Nitrogen (blue), Sulfur (yellow), Phosphorus (orange), Oxygen (red), and Platinum (violet). Hydrogen atoms are omitted for simplicity. *(A higher resolution / colour version of this figure is available in the electronic copy of the article).*

angles (88.96°-93.99°) are also deviating from (90°). This deviation arose from the participation of the bulky formamidine ligands in coordination. The calculated bond length of Pt-O(2.02°-2.06°) and Pt-N (1.97°-2.05°) were compared with the published Pt(II) complexes and were found to be consistent (Pt-O: 2.00°-2.03°, Pt-N: 2.01°-2.02°) [14, 35]. The atomic charges explain the possible donor and acceptor property of atoms [36]. The higher charge density has been found to be assigned on ligand's nitrogen atoms, which explains their donor properties. The platinum as the positive core acts as the acceptor. The back donation is contingent on the higher negative charges of nitrogen atoms in complexes compared with ligands. This can be reasoned as MLCT from the platinum to the π*-orbitals of ligands. The positive charges on the sulfur atoms in $\mathbf{L_1}$ (+ 0.249) and complex (**1**) (+ 0.282), for example, make it hard to act as a binding site [15]. The complexes were found to be more polarized (9.74-18.13 Debye) than ligands (1.93-4.90 Debye) [13, 15, 16, 37]. The calculated electronic energies of the complexes and their dipole moments are given in Table **S3**. Natural Bond Orbital (NBO) calculations were conducted using the B3LYP / LanL2DZ basis set. Accordingly, for complex (**1**), the platinum electronic configuration is :[Xe] $6s^{0.49}$ $5d^{8.55}$ $6p^{0.27}$ $6d^{0.02}$ $7p^{0.01}$, 68 core electrons, 9.34 valence electrons, and 0.026 Rydberg electrons, which sum to 77.37 electrons and +0.68e charge on Pt atom. The occupancies of Pt 5d orbitals are d_{xy} 1.958; d_{xz} 1.872; d_{yz} 1.785; $d_{x^2-y^2}$ 1.050 and d_{z^2} 1.886. The 5d-electron populations of 8.551 correspondings to the oxidation state Pt(II) is covenant with ligand to d_{Pt} electron transfer. The occupancy of the $d_{x^2-y^2}$ may be explained on the base of the possibility of electron transfer from ligand to metal (LMCT). Similar trends are

shown by complexes (**2-4**) with Pt 5*d* populations (8.186-8.561) confirming the ligand to metal electron transfer. The electronic energies of the complexes (-1726 to -2279 a.u.) are more stable than ligands (-949 to -397) [13, 15, 16, 38]. The calculated HOMO and LUMO energies are given in Table **S3**. The hardness (η) values are calculated from the ionization energies (I) and electron affinities (A) as (η = (I-A) / 2) and (I-A) are equal to the energy difference between the HOMO-LUMO energies. The higher the values of (I-A) the harder are the molecules and vice versa [39, 40]. The η values and ΔE (HOMO-LUMO) are arranged in Table **S3**. The transition is much easy in the complexes than in the ligands; ΔE of complexes is (0.118-0.145) and of ligands is (0.106-0.310) [38]. Hence, the complexes (**1-4**) are more soft (η = (0.059-0.072) compared with the ligands (0.053-0.155) [37]. The stability of ligands and complexes is indicated from the negative values of HOMO and the LUMO as well as their energy separation [38, 39]. The isodensity surface graphs of the HOMO and LUMO for complexes are represented by complex (**2**); Fig. (**S1**). The electron densities in $\mathbf{L_2}$ are localized on the benzimidazole part, which may point to a mixed π→π* and n→π* transition [36]; Fig. (**S1**). The molecular electrostatic potential (MEP) has been calculated and is shown in Fig. (**S2**), the red and blue sections indicate electrophilic and nucleophilic reactivity; respectively. The nitrogen atoms of the ligands; with their negative (red) regions are the responsive sites for the electrophilic attack [40]. Contrarywise, the negative regions (red) in complexes are largely found in the oxygen atoms of pyrophosphate ligand.

3.8. Cytotoxicity

Cytotoxicity of complexes (**1,2,4**) was tested (*in vitro*) in DMSO against the liver carcinoma cell line (HepG-2), human breast adenocarcinoma (MCF-7), and colon carcinoma cell line (HTC-116) using cisplatin and doxorubicin as references. The experiment was conducted in triplicate and the average results are considered, the results are shown in Fig. (**7**). The IC50 values of the complexes were deduced in micromoles (concentration in microgram at 50% viability/molar mass of complex) and tabulated in Table **8**. The complexes have a noticeable cytotoxicity with IC50 (μM) for MCF-7 (0.035-0.144), HepG-2 (0.063-0.163) and HCT-116 (0.042-0.187) cell lines. [Pt(L4)PPi].7/2H2O (4) has the best IC50 values ranged (0.035 to0.063) μM against the used cell lines which shows that the complexes are promising antitumor candidates for further studies.

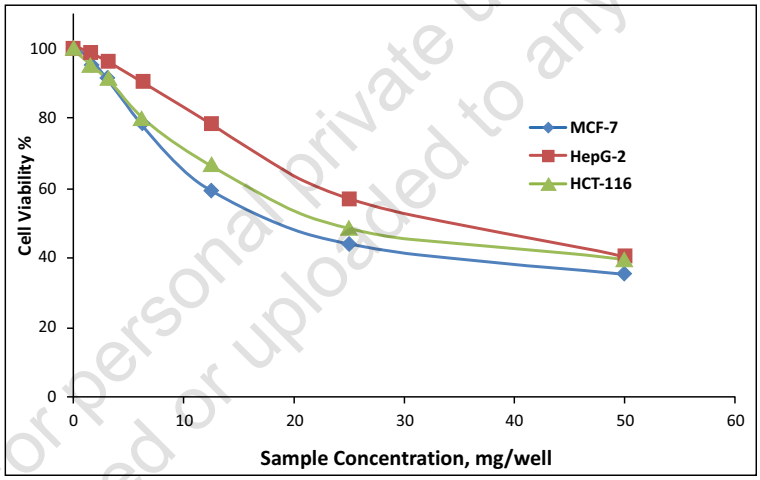

Fig. (7). Cell viability of [Pt(L_4)PPi].7/2H_2O (**4**) against HepG-2, MCF-7, and HCT-116 cell lines. *(A higher resolution / colour version of this figure is available in the electronic copy of the article).*

Table 8. IC_{50} values of for the ligands and some Pt(II) complexes.

Complex	IC_{50} (μM)		
	MCF-7	HCT-116	HepG-2
L_1	0.024±0.007	0.025±0.011	0.040±0.009
L_2	0.050±0.012	0.115±0.015	0.051±0.017
L_3	0.168±0.007	0.150±0.003	0.222±0.011
L_4	0.011±0.013	0.012±0.019	0.006±0.012
[Pt(L_1)PPi].2H_2O (1)	0.144±0.017	0.154±0.009	0.168±0.015
[Pt(L_2)PPi].2H_2O (2)	0.131±0.015	0.187±0.014	0.154±0.016
[Pt(L_4)PPi].7/2H_2O (4)	0.035±0.013	0.042±0.008	0.063±0.006
Doxorubicin	0.008±0.011	0.008±0.018	0.008±0.006

CONCLUSION

Ternary platinum (II) complexes with formamidine and pyrophosphate have been prepared and characterized. The complexes (**1-4**) have been proven to be diamagnetic with distorted square planar. The stability of the complexes was inferred from the negative HOMO and LUMO's energies. The thermal stability of complexes (**1-4**) has been inferred from their high total activation energies (368-660 kJ mol^{-1}). The complexes showed noticeable cytotoxicity (IC_{50} (μM): MCF-7 (0.035-0.144), HepG-2 (0.063-0.163) and HCT-116 (0.042-0.187). The complexes are considered as promising antitumor candidates for further application.

ETHICS APPROVAL AND CONSENT TO PARTICIPATE

Not applicable.

HUMAN AND ANIMAL RIGHTS

No animals/humans were used for studies that are the basis of this research.

CONSENT FOR PUBLICATION

Not applicable.

AVAILABILITY OF DATA AND MATERIALS

The authors confirm that the data supporting the findings of this study are available within the article.

FUNDING

None.

CONFLICT OF INTEREST

The authors declare no conflict of interest, financial or otherwise.

ACKNOWLEDGEMENTS

Declared none.

SUPPLEMENTARY MATERIAL

Supplementary material is available on the publisher's website along with the published article.

REFERENCES

[1] Tabrizi, L.; Chiniforoshan, H. New platinum(II) complexes of CCC-pincer N-heterocyclic carbene ligand: Synthesis, characterization, cytotoxicity and antileishmanial activity. *J. Organomet. Chem.,* **2016**, *818*, 98. http://dx.doi.org/10.1016/j.jorganchem.2016.06.013

[2] Lebwohl, D.; Canetta, R. Clinical development of platinum complexes in cancer therapy: an historical perspective and an update. *Eur. J. Cancer,* **1998**, *34*(10), 1522-1534. http://dx.doi.org/10.1016/S0959-8049(98)00224-X PMID: 9893623

[3] Wong, E.; Giandomenico, C.M. Current status of platinum-based antitumor drugs. *Chem. Rev.,* **1999**, *99*(9), 2451-2466. http://dx.doi.org/10.1021/cr980420v PMID: 11749486

[4] Kostova, I. Platinum complexes as anticancer agents. *Recent Pat. Anticancer Drug Discov.,* **2006**, *1*(1), 1-22. http://dx.doi.org/10.2174/157489206775246458

[5] Hall, M.D.; Mellor, H.R.; Callaghan, R.; Hambley, T.W. Basis for design and development of platinum(IV) anticancer complexes. *J. Med. Chem.,* **2007**, *50*(15), 3403-3411. http://dx.doi.org/10.1021/jm070280u PMID: 17602547

[6] Monroe, J.D.; Hruska, H.L.; Ruggles, H.K.; Williams, K.M.; Smith, M.E. Anti-cancer characteristics and ototoxicity of platinum(II) amine complexes with only one leaving ligand. *PLoS One,* **2018**, *13*(3), e0192505. http://dx.doi.org/10.1371/journal.pone.0192505 PMID: 29513752

[7] Spinu, C.; Pleniceanu, M.; Tigae, C. Biologically active new Fe(II), Co(II), Ni(II), Cu(II), Zn(II) and Cd(II) complexes of N-(2-thienylmethylene)methanamine. *J. Serb. Chem. Soc.,* **2008**, *73*, 415-421. http://dx.doi.org/10.2298/JSC0804415S

[8] Hung, W.C.; Lin, C.C. Preparation, characterization, and catalytic studies of magnesium complexes supported by NNO-tridentate Schiff-base ligands. *Inorg. Chem.,* **2009**, *48*(2), 728-734. http://dx.doi.org/10.1021/ic801397t PMID: 19072296

[9] Cubo, L.; Pizarro, A.M.; Quiroga, A.G.; Salassa, L.; Navarro-Ranninger, C.; Sadler, P.J. Photoactivation of trans diamine platinum complexes in aqueous solution and effect on reactivity towards nucleotides. *J. Inorg. Biochem.,* **2010**, *104*(9), 909-918. http://dx.doi.org/10.1016/j.jinorgbio.2010.04.009 PMID: 20546905

[10] Farrer, N.J.; Woods, J.A.; Salassa, L.; Zhao, Y.; Robinson, K.S.; Clarkson, G.; Mackay, F.S.; Sadler, P.J. A potent trans-diimine platinum anticancer complex photoactivated by visible light. *Angew. Chem. Int. Ed. Engl.,* **2010**, *49*(47), 8905-8908. http://dx.doi.org/10.1002/anie.201003399 PMID: 20677309

[11] Fanelli, M.; Formica, M.; Fusi, V.; Giorgi, L.; Micheloni, M.; Paoli, P. New trends in platinum and palladium complexes as antineoplastic agents. *Coord. Chem. Rev.,* **2016**, *310*, 41-79. http://dx.doi.org/10.1016/j.ccr.2015.11.004

[12] Hoffmeister, B.R.; Adib-Razavi, M.S.; Jakupec, M.A.; Galanski, M.; Keppler, B.K. Diamminetetrakis(carboxylato)platinum(IV) complexes--synthesis, characterization, and cytotoxicity. *Chem. Biodivers.,* **2012**, *9*(9), 1840-1848. http://dx.doi.org/10.1002/cbdv.201200019 PMID: 22976974

[13] Soliman, A.A.; Alajrawy, O.I.; Attabi, F.A.; Linert, W. New dinuclear palladium(II) complexes with formamidine and bridged pyrophosphate ligands. *New J. Chem.,* **2016**, *40*, 8342-8354. http://dx.doi.org/10.1039/C6NJ01262K

[14] Mishur, R.J.; Zheng, C.; Gilbert, T.M.; Bose, R.N. Synthesis, X-ray crystallographic, and NMR characterizations of platinum(II) and platinum(IV) pyrophosphato complexes. *Inorg. Chem.,* **2008**, *47*(18), 7972-7982. http://dx.doi.org/10.1021/ic800237a PMID: 18693681

[15] Soliman, A.A.; Alajrawy, O.I.; Attabi, F.A.; Shaaban, M.R.; Linert, W. New formamidine ligands and their mixed ligand palladium(II) oxalate complexes: Synthesis, characterization, DFT calculations and *in vitro* cytotoxicity. *Spectrochim. Acta A Mol. Biomol. Spectrosc.,* **2016**, *152*, 358-369. http://dx.doi.org/10.1016/j.saa.2015.07.076 PMID: 26232580

[16] Soliman, A.A.; Alajrawy, O.I.; Attabi, F.A.; Shaaban, M.R.; Linert, W. New binary and ternary platinum(II) formamidine complexes: Synthesis, characterization, structural studies and *in-vitro* antitumor activity. *J. Mol. Struct.,* **2016**, *1115*, 17-32. http://dx.doi.org/10.1016/j.molstruc.2016.02.073

[17] Soliman, A.A.; Meseha, M.A.; Sayed, A.; Abou-Hussein, A.; Linert, W. Cobalt and copper complexes with formamidine ligands: Synthesis, Crystal x-ray study, DFT calculations, and Cytotoxicity. *Polyhedron,* **2019**, *161*, 213-221. http://dx.doi.org/10.1016/j.poly.2018.12.020

[18] Soliman, A.A.; Attaby, F.A.; Alajrawy, O.I.; Majeed, S.R.; Sahin, C.; Varlikli, C. Soluble cytotoxic ruthenium(II) complexes with 2-hydrazinopyridine. *Russ. J. Inorg. Chem.,* **2019**, *64*(6), 742-754. http://dx.doi.org/10.1134/S0036023619060020

[19] Soliman, A.A.; Attaby, F.A.; Alajrawy, O.I.; Majeed, S.R. Soluble ruthenium(II) with 3,4-diaminobenzoic acid complexes: Preparation, thermal study, theoretical calculations and *in vitro* cytotoxic activity. *J. Therm. Anal. Calorim.,* **2019**, *135*, 2457-2473. http://dx.doi.org/10.1007/s10973-018-7405-6

[20] Mosmann, T. Rapid colorimetric assay for cellular growth and survival: application to proliferation and cytotoxicity assays. *J. Immunol. Methods,* **1983**, *65*(1-2), 55-63. http://dx.doi.org/10.1016/0022-1759(83)90303-4 PMID: 6606682

[21] Nakamoto, N. *Infrared and Raman Spectra of Inorganic and Coordination Compounds*; Wiley: New York, **1986**.

[22] Marino, N.; Ikotun, O.F.; Julve, M.; Lloret, F.; Cano, J.; Doyle, R.P. Pyrophosphate-mediated magnetic interactions in Cu(II) coordination complexes. *Inorg. Chem.,* **2011**, *50*(1), 378-389. http://dx.doi.org/10.1021/ic1020884 PMID: 21114311

[23] Makhkhas, Y.; Aqdim, S.; Sayouty, E. Study of Sodium-Chromium-Iron-Phosphate Glass by XRD, IR, Chemical Durability and SEM. *J. Mater. Sci. Chem. Eng,* **2013**, *1*, 1-6. http://dx.doi.org/10.4236/msce.2013.13001

[24] Bush, R.P. Recovery of platinum group metals from high level radioactive waste. *Platin. Met. Rev.,* **1991**, *35*(4), 202-208.

[25] Lever, A.B.P. *Inorganic electronic spectroscopy,* 2nd ed; Elsevier: Amsterdam, Holland, **1984**, p. 544.

[26] Pellacani, G.C.; Malavasi, W.D.D. Palladium(II) complexes with N,N′ -dimethyldithiomalonamide. *J. Inorg. Nucl. Chem.,* **1975**, *37*, 477-481. http://dx.doi.org/10.1016/0022-1902(75)80359-9

[27] Housecroft, C.E.; Sharpe, A.G. *Inorganic Chemistry,* 2nd ed; Pearson: England, **2005**, p. 579.

[28] Horowitz, H.H.; Metzger, G.A. New analysis of thermogravimetric traces. *Anal. Chem.,* **1963**, *35*(10), 1464-1468. http://dx.doi.org/10.1021/ac60203a013

[29] Coats, A.W.; Redfern, J.P. Kinetic Parameters from Thermogravimetric Data. *Nature,* **1964**, *201*, 68-69. http://dx.doi.org/10.1038/201068a0

[30] Soliman, A.A.; Samir, M.E.; Omyma, A.A.M. Thermal study of chromium and molybdenum complexes with some nitrogen and nitrogen-oxygen donors ligands. *J. Therm. Anal. Calorim.,* **2006**, *83*(2), 385-392. http://dx.doi.org/10.1007/s10973-005-7009-9

[31] Soliman, A.A.; Khattab, M.M.; Ramadan, R.M. Synthesis and characterization of new chromium, molybdenum and tungsten complexes of 2-[2-(methylaminoethyl)] pyridine. *Transit. Met. Chem.,* **2007**, *32*, 325-331. http://dx.doi.org/10.1007/s11243-006-0171-5

[32] Ali, S.A.; Soliman, A.A.; Aboli, M.M.; Ramadan, R.M. Chromium, molybdenum and ruthenium complexes of 2-hydroxyacetop henone schiff bases. *J. Coord. Chem.,* **2002**, *55*(10), 1161-1170. http://dx.doi.org/10.1080/0095897021000023509

[33] Dunning, T.H., Jr; Hay, P.J. *Modern Theoretical Chemistry,* 3rd ed; Plenum: New York, **1976**, Vol. *3*, pp. 1-28.

[34] Andrae, D.; Häußermann, U.; Dolg, M.; Stoll, H.; Preuß, H. Energy-adjustedab initio pseudopotentials for the second and third row transition elements. *Theor. Chem. Acc.,* **1990**, *77*, 123-141. http://dx.doi.org/10.1007/BF01114537

[35] Bakalova, A.; Vaabnov, H.; Stanchev, S.; Ivanov, D.; Jensen, F. DFT study of the structure and spectral behavior of new Pt(II) complexes with 5-methyl-5(4-pyridyl) hydantoin. *Int. J. Quantum Chem.,* **2009**, *109*(4), 826-836. http://dx.doi.org/10.1002/qua.21890

[36] Adamo, C. Toward reliable density functional methods without adjustable parameters: The PBE0 model. *J. Chem. Phys.,* **1999**, *110*, 6158. http://dx.doi.org/10.1063/1.478522

[37] Akçay, H.T.; Bayrak, R. Computational studies on the anastrozole and letrozole, effective chemotherapy drugs against breast cancer. *Spectrochim. Acta A Mol. Biomol. Spectrosc.,* **2014**, *122*, 142-152. http://dx.doi.org/10.1016/j.saa.2013.11.028 PMID: 24309175

[38] Chattaraj, P.K.; Giri, S. Stability, reactivity, and aromaticity of compounds of a multivalent superatom. *J. Phys. Chem. A,* **2007**, *111*(43), 11116-11121. http://dx.doi.org/10.1021/jp0760758 PMID: 17915847

[39] Sabounchei, S.J.; Shahriary, P.; Salehzadeh, S.; Gholiee, Y.; Nematollahi, D.; Chehregani, A.; Amani, A.; Afsartala, Z. Pd(II) and Pd(IV) complexes with 5-methyl-5-(4-pyridyl)hydantoin: synthesis, physicochemical, theoretical, and pharmacological investigation. *Spectrochim. Acta A Mol. Biomol. Spectrosc.,* **2015**, *135*, 1019-1031. http://dx.doi.org/10.1016/j.saa.2014.08.002 PMID: 25171052

[40] Liu, F.; Zhou, Z.; Gou, S.; Zhao, J.; Chen, F. Synthesis and antiproliferative activity of (1R,2R)-N1-(2-butyl)-1,2-cyclohexanediamine platinum(II) complexes with malonate derivatives. *J. Coord. Chem.,* **2004**, *67*(17), 2858-2866. http://dx.doi.org/10.1080/00958972.2014.951638